Many-body Majorana-like zero modes without gauge symmetry breaking

V. Vadimov,[1, 2, 3] T. Hyart,[4, 5] J. L. Lado,[4] M. Möttönen,[1, 6] and T. Ala-Nissila[2, 7]

[1]*QCD Labs, QTF Centre of Excellence, Department of Applied Physics,*
Aalto University, P.O. Box 13500,FI-00076 Aalto, Espoo, Finland
[2]*MSP Group, QTF Centre of Excellence, Department of Applied Physics,*
Aalto University, P.O. Box 11000, FI-00076 Aalto, Espoo, Finland
[3]*Institute for Physics of Microstructures, Russian Academy of Sciences, 603950 Nizhny Novgorod, GSP-105, Russia*
[4]*Department of Applied Physics, Aalto University, FI-00076 Aalto, Espoo, Finland*
[5]*International Research Centre MagTop, Institute of Physics,*
Polish Academy of Sciences, Al. Lotników 32/46, 02-668 Warsaw, Poland
[6]*VTT Technical Research Centre of Finland Ltd.,*
QTF Center of Excellence, P.O. Box 1000, FI-02044 VTT, Finland
[7]*Interdisciplinary Centre for Mathematical Modelling, Department of Mathematical Sciences,*
Loughborough University, Loughborough LE11 3TU, UK
(Dated: November 13, 2020)

Topological superconductors represent one of the key hosts of Majorana-based topological quantum computing. Typical scenarios for one-dimensional topological superconductivity assume a broken gauge symmetry associated to a superconducting state. However, no interacting one-dimensional many-body system is known to spontaneously break gauge symmetries. Here, we show that zero modes emerge in a many-body system without gauge symmetry breaking and in the absence of superconducting order. In particular, we demonstrate that Majorana zero modes of the symmetry-broken superconducting state are continuously connected to these zero-mode excitations, demonstrating that zero-bias anomalies may emerge in the absence of gauge symmetry breaking. We demonstrate that these many-body zero modes share the robustness features of the Majorana zero modes of symmetry-broken topological superconductors. We introduce a bosonization formalism to analyze these excitations and show that a ground state analogous to a topological superconducting state can be analytically found in a certain limit. Our results demonstrate that robust Majorana-like zero modes may appear in a many-body systems without gauge symmetry breaking, thus introducing a family of protected excitations with no single-particle analogs.

I. INTRODUCTION

Superconductivity in topological quantum materials has become one of the most fertile topics in modern condensed matter physics [1, 2]. The search for topological superconductors has been motivated by the emergence of topological excitations, known as Majorana zero modes [3], and by their potential for topological quantum computing [4–13]. A variety of solid-state materials have been explored in recent years with the goal of engineering Majorana bound states, including superconducting nanowires [14–22], atomically engineered chains [23–26], topological insulators [27–31], phase-controlled Josephson junctions [32, 33], helical quantum Hall edge states of graphene [34] with controllable magnetic [35, 36] and superconducting gaps, antiferromagnetic topological superconductors [37, 38], and van der Waals heterostructures [39]. These different platforms rely on the engineering of a specific kind of an effective p-wave superconducting state, the non-trivial topological properties of which give rise to the emergence of Majorana zero modes [40].

Majorana bound states and unconventional superconductors in general rely on a single-particle description of the effective excitations. In particular, conventional proposals for Majorana bound states in topological superconductors rely on explicitly broken gauge symmetry which is associated with the existence of a non-zero superfluid order parameter [40].

In this scenario, the existence of Majorana bound states in the presence of particle–particle interactions has been established in terms of a renormalization of the single-particle mean-field parameters [41–45]. Although additional subtle many-body effects are prone to appear in this regime [46–49], the Majorana zero remain to exist.

However, the scenario for systems lacking symmetry breaking is distinctively different [50–59]. Namely, particle–particle interactions cannot be reinterpreted as a renormalization of single-particle terms as in a symmetry broken state. For typical single-particle models of topological superconductivity, the pairing term explicitly breaks the gauge symmetry since the term is not $U(1)$ gauge symmetric. A finite pairing term is a hallmark of superconductivity, and thus such symmetry breaking is natural for proposals that involve three-dimensional superconductors [60]. However, for a purely one-dimensional (1D) system, the situation is dramatically different, as spontaneous symmetry breaking with finite pairing does not take place [61, 62]. In particular, interacting 1D models have a ground state that is gauge symmetric with a vanishing expectation value of superconducting pairing [61, 62], and consequently their effective single-particle Hamiltonian does not host Majorana zero modes [40, 60]. Thus, whether or not Majorana zero modes may appear in the absence of gauge symmetry breaking is a major outstanding question.

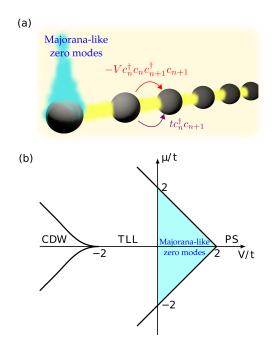In this work, we demonstrate that robust zero modes

FIG. 1. (a) Schematic illustration of the interacting one-dimensional model we study. The Majorana-like zero energy mode at the left edge of the chain is highlighted with cyan color. The fermionic creation and annihilation operators at site n (grey sphere) are denoted by $\hat{c}_n^\dagger$ and $\hat{c}_n$, respectively. The strength of the particle hopping between neighboring sites (yellow color) is given by t, and V describes the strength of the interactions between the fermions. (b) The phase diagram of the Hamiltonian (1) at zero temperature. Here, μ denotes the chemical potential. Regions corresponding to a phase separation (PS), Tomonaga–Luttinger liquid (TLL), and charge density wave (CDW) appear in addition to Majorana-like zero modes (cyan color).

appear in a 1D many-body model without gauge symmetry breaking. The model we focus on would give rise to a topological superconductor at the mean-field level if the gauge symmetry were explicitly broken. We demonstrate that no such gauge symmetry breaking is required for the emergence of Majorana-like zero modes, establishing a peculiar paradigm of topological quantum many-body excitations with no single-particle analog. Despite their fundamental differences to Majorana zero modes, we demonstrate that these two types of many-body excitations share many properties, including robustness to perturbations and disorder.

Our manuscript is organized as follows. In Sec. II, we introduce the many-body model, highlighting the emergence of zero-mode resonances. In Sec. III, we demonstrate the robustness of the zero modes to a variety of perturbations. In Sec. IV, we show the connection between these resonant zero modes and Majorana bound states. In Sec. V, we demonstrate the emergence of the edge modes from a continuum bosonization formalism. Section VI summarizes our results and Appendices A–C discuss some technical details such as critical points,

Green's functions, and persistent current in a ring.

II. ZERO MODES IN QUANTUM MANY-BODY CHAINS

We study a 1D chain of L spinless fermions with interactions between the neighboring sites as illustrated in Fig. 1(a). The system is described by the following Hamiltonian:

$$\hat{H}_I = -t \sum_{j=1}^{L-1} \left(\hat{c}_{j+1}^\dagger \hat{c}_j + \hat{c}_j^\dagger \hat{c}_{j+1} \right) - \mu \sum_{j=1}^{L} \hat{c}_j^\dagger \hat{c}_j$$
$$- V \sum_{j=1}^{L-1} \left(\hat{c}_{j+1}^\dagger \hat{c}_{j+1} - \frac{1}{2} \right) \left(\hat{c}_j^\dagger \hat{c}_j - \frac{1}{2} \right), \quad (1)$$

where t is the strength of the particle hopping between neighboring sites, $\hat{c}_j^\dagger$ and $\hat{c}_j$ are the fermionic creation and annihilation operators at site j, respectively, μ is the chemical potential, and V is the strength of the interactions between the fermions. Such a system can be mapped onto a spin-1/2 anisotropic XXZ chain in a longitudinal field using the Jordan–Wigner transformation, resulting in

$$\hat{H}_I = \sum_{j=1}^{L-1} \left[2t \left(\hat{s}_j^x \hat{s}_{j+1}^x + \hat{s}_j^y \hat{s}_{j+1}^y \right) - V \hat{s}_j^z \hat{s}_{j+1}^z \right] - \mu \sum_{j=1}^{L} \hat{s}_j^z,$$

where $\{\hat{s}_j^\alpha\}_{\alpha=x,y,z}$ denote the spin-1/2 operators for site j. This model is integrable by the means of the Bethe ansatz [63, 64]. The resulting phase diagram at zero temperature and otherwise in the thermodynamic limit is shown in Fig. 1(b) [65]. We focus on the region of the diagram corresponding to the attractive interactions between the fermions $V > 0$, where two different phases exist. Phase separation takes place at $|\mu| > 2t - V$ where the ground sate corresponds, depending on the sign of μ, to the vacuum state or to the completely filled band. In this phase, zero-energy modes which mix the number of particles are known to exist [66]. The other phase corresponds to the Tomonaga–Luttinger liquid [67–69] which is our main focus here. Remarkably, we have been able to explicitly construct the ground state at the critical point $V = 2t$, $\mu = 0$ as shown in Appendix A. At this point it appears to be $L+1$ times degenerate, where the different degenerate states correspond to the different numbers of particles.

Treated within the mean-field approximation such a model gives rise to the well-known Kitaev model described by the Hamiltonian

$$\hat{H}_K = -t \sum_{j=1}^{L-1} \left(\hat{c}_{j+1}^\dagger \hat{c}_j + \hat{c}_j^\dagger \hat{c}_{j+1} \right) - \mu \sum_{j=1}^{L} \hat{c}_j^\dagger \hat{c}_j +$$
$$\sum_{j=1}^{L-1} \left(\Delta_j \hat{c}_{j+1}^\dagger \hat{c}_j^\dagger + \Delta_j^* \hat{c}_j \hat{c}_{j+1} \right), \quad (2)$$
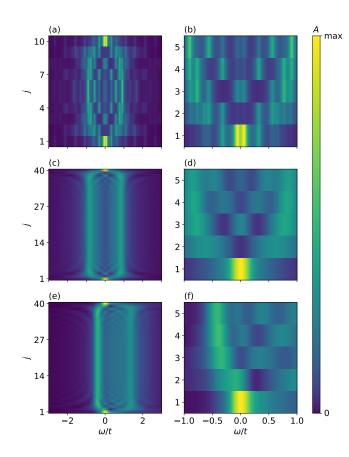
FIG. 2. Local density of states as a function of frequency and the site of the chain for (a,b) $L = 10$, $\mu = 0$ (c,d) $L = 40$, $\mu = 0$ (e,f) $L = 40$, $\mu = -0.2t$. Panels (b,d,f) show the maps of the local density of states $A(j,\omega)$ zoomed to the edge of the chain from the corresponding panels (a,c,e) . The interaction strength is $V = 1.5t$. The panels (a,b) have been obtained using exact diagonalization of the Hamiltonian (1) and the others are obtained using the KPM-MPS method.

FIG. 3. (a) Scaling of the peak splitting with L. (b) Dependence of the prefactor C on the interaction strength V. The calculations are performed using MPS algorithm with $\mu = 0$.

A. Local density of states

The local density of states, or the spectral function, of the chain is defined as

$$
\begin{aligned}
A(j,\omega) = \langle\Psi_0|\hat{c}_j\delta(\omega - \hat{H} + E_0)\hat{c}_j^\dagger + \\
\hat{c}_j^\dagger\delta(\omega + \hat{H} - E_0)\hat{c}_j|\Psi_0\rangle = \\
\sum_m \Big[|\langle\Psi_0|\hat{c}_j|\Psi_m\rangle|^2\delta(\omega - E_m + E_0) + \\
|\langle\Psi_0|\hat{c}_j^\dagger|\Psi_m\rangle|^2\delta(\omega - E_0 + E_m)\Big], \quad (3)
\end{aligned}
$$

where $|\Psi_0\rangle$ is the ground state with energy E_0 and $|\Psi_m\rangle$ are all the eigenstates of the system corresponding to energies E_m. The spectral function can be evaluated using exact diagonalization of the Hamiltonian for the short chains or using a kernel polynomial method with matrix product states (KPM-MPS) [70–76] for the reasonably long chains.

The results of our calculations are shown in Fig. 2. We observe clear zero-bias peaks at the edges of the chain, corresponding to Majorana-like zero modes. We find that these zero-energy peaks appear for all considered chemical potentials μ. Similarly to Majorana edge modes, the peaks split for short chains as shown in Fig. 2(b), stemming from the hybridization of the excitations at the opposite edges. With increasing chain length L, the edge peaks move towards zero energy, constituting a zero-energy resonance in the limit $L \to \infty$. Next, we systematically examine how the splitting of these edge modes depends on the system size. Interestingly, their behavior is different from that of Majorana zero modes in topological superconductors.

B. Peak scaling

The nature of the above-found edge modes can be studied by inspecting the scaling properties of the peak splitting. From the series expression in Eq. (3), we observe that the the peaks peaks are located at energies $\pm[E_0(N_0 \pm 1) - E_0]$, where $E_0(N)$ is the energy of the

where the superconducting order parameter Δ_j is determined self-consistently as $\Delta_j = V\langle\hat{c}_j\hat{c}_{j+1}\rangle$. The Kitaev model spontaneously breaks the gauge symmetry which is present in the original model (1). For $L \gg t/|\Delta|$ this model hosts Majorana zero modes localized at the ends of the chain [40] whereas the other excited states are separated from the ground state by $|\Delta|$ in the bulk of the chain.
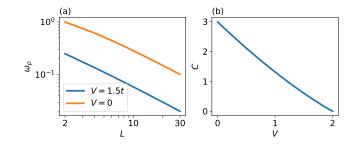
ground state in the subspace with N particles and N_0 is the number of particles in the global ground state of the system. Thus the peak splitting ω_{p} appears to be equal to $[E_0(N_0 + 1) + E_0(N_0 - 1)]/2 - E_0$ and its dependence of the chain length L is shown in Fig. 3(a). For comparison, Fig. 3(a) also shows the same parameter for a non-interacting chain, which corresponds to the level spacing at the Fermi energy. One can see that the splitting scales as $C(V)/L$, which is in contrast to the mean-field case where the splitting of the Majorana peaks decays exponentially with the length of the chain. In the case of conventional Majorana states, the exponential dependence arises because of two reasons. First, the bulk of the system has a gap stemming from the finite pairing. As Majorana zero modes are located inside the gap in the bulk of the system, they need to decay exponentially, which gives rise to hybridization between zero modes that decays exponentially with the system size. Secondly, the induced superconductivity may be thought as arising from coupling to an infinite superconductor (which does not have charging energy). Since the Majorana wire can exchange Cooper pairs with the infinite superconductor, there is no energy cost for adding particles to the system. As a result of these two effects, the states with N_0 and $N_0 \pm 1$ particles are degenerate up to the hybridization energy, which decays exponentially with the system size. In stark contrast, the present system is different from the conventional Majorana states in both ways. First, it does not have a gap stemming from the pairing, and the bulk remains gapless. As a result, the Majorana-like resonances do not have an exponential localization in the edge but rather power-law, and thus, the hybridization energy decays as a power-law with the system size. Secondly, we are considering a finite system which cannot exchange particles with an infinite superconductor, so that adding particles to the system costs energy $\propto 1/L$, and therefore a splitting $\omega_p \propto 1/L$ would be obtained independently on the type of localization of the end modes (see also Sec. V). Both contributions are fully included in our calculations. Dependence of the scaling coefficient $C(V)$ on the interaction strength is shown in Fig. 3(b). One can see that it decays almost linearly to 0 at the critical point $V = 2t$.

III.   ROBUSTNESS OF THE ZERO MODES TO PERTURBATIONS

A paradigmatic property of topological states in general, and Majorana bound states in particular, is their robustness towards perturbations in the Hamiltonian. To this end we study robustness of the peaks with respect to perturbations that break the integrability of the model. We consider three different types of perturbations: second-neighbor hopping, second-neighbor interactions, and on-site disorder. These perturbations are
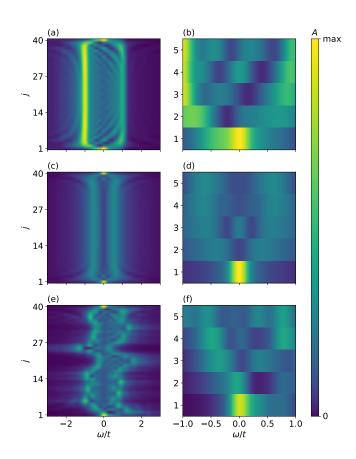

FIG. 4. The local density of states as a function of frequency and the site of the chain for perturbed systems. The perturbations are (a,b) second-neighbor hopping, (c,d) second-neighbor interaction, and (e,f) on-site disorder. The parameters are $L = 40$, $V = 1.5t$, $\mu = 0$, (a,b) $t' = -0.2t$, (c,d) $V' = 0.4t$, (e, f) $W = 0.5t$. It can be seen that in all the cases there are strong zero-modes at the edge demonstrating the robustness of these states.

described by the following Hamiltonians, respectively:

$$\hat{H}_{2\mathrm{nh}} = -t' \sum_{j=1}^{L-2} \left(\hat{c}_{j+2}^{\dagger} \hat{c}_j + \hat{c}_j^{\dagger} \hat{c}_{j+2} \right); \qquad (4)$$

$$\hat{H}_{2\mathrm{ni}} = -V' \sum_{j=1}^{L-2} \left(\hat{c}_{j+2}^{\dagger} \hat{c}_{j+2} - \frac{1}{2} \right) \left(\hat{c}_j^{\dagger} \hat{c}_j - \frac{1}{2} \right), \qquad (5)$$

$$\hat{H}_d = \sum_{j=1}^{L} u_j \hat{c}_j^{\dagger} \hat{c}_j, \qquad (6)$$

where t', V' are the parameters controlling the second neighbor hopping and interactions, respectively, and u_j is the on-site potential which is a random number with amplitude W in the range $[-W, W]$. The distributions of local density of states for these types of perturbations are shown in the Fig. 4. For all cases here we find that weak perturbations do not affect the existence of the edge states.
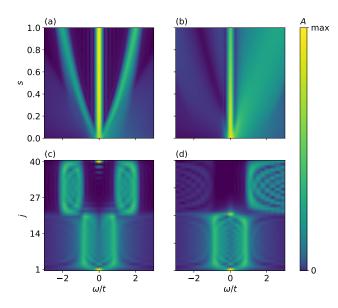
FIG. 5. (a,b) Local density of states at the first site as a function of parameter s and frequency calculated for the Hamiltonian (7). Here $L = 40$, $V = 1.5t$, $\Delta = t$, (a) $\mu = -0.2t$, $\tilde{\mu}(s) = 0$ and (b) $\tilde{\mu}(s)$ is adjusted in such a way that $\langle N \rangle (s)/L = 1/4$. Panels (c,d) show the local density of states for each site in a heterosjunction between a topological superconductor and the interacting model (c), and between a trivial superconductor and the interacting model (d). The parameters are $L' = 20$, $\Delta = 0.5t$, $\mu = 0$, (c) $\mu' = 0$, (d) $\mu' = 3$.

IV. CONNECTION TO A TOPOLOGICAL SYMMETRY BROKEN SUPERCONDUCTOR

So far we have focused on the quantum disordered state, showing that the interacting gapless gas shows topological excitations sharing the robust properties of Majorana zero modes. While such similarity is suggestive, a stronger insight in the relation between the two can be obtained by demonstrating that the two types of excitations can be smoothly connected. In this section we demonstrate that the Majorana-like zero modes can be transformed into true Majorana bound states by performing an adiabatic connection between the two. For this purpose we introduce a parametric family of Hamiltonians

$$\hat{H}(s) = (1-s)\hat{H}_I + s\hat{H}_K - \tilde{\mu}(s)\hat{N}, \ 0 \leqslant s \leqslant 1, \quad (7)$$

which smoothly transform from the interacting chain to a topological superconductor with gauge symmetry breaking by changing of the parameter s. In particular, for $s = 0$ Eq. (7) becomes the many-body Hamiltonian studied in previous sections, whereas for $s = 1$ Eq. (7) is a single-particle Hamiltonian for a topological superconductor. Therefore, changing the parameter s allows tracking the evolution from the Majorana-like modes without symmetry breaking to Majorana modes with symmetry breaking. The chemical potential $\tilde{\mu}(s)$ is

defined to control the total number of particles throughout the path.

The spectral function at the edge of the chain as a function of the parameter s is shown in Fig. 5. When the chemical potential μ does not exceed the transition value $2t - V$ in absolute value and does not depend on the parameter $\tilde{\mu}(s) = 0$, the bulk gap exactly closes at $s = 0$, i.e. in the fully interacting model (see Fig. 5(a)). Another way to connect the fully interacting model to the Kitaev chain is to keep the mean number of particles $\langle N \rangle (s)$ constant with varying the parameter s. This case is shown in Fig. 5(b), which is qualitatively similar to the case of the constant chemical potential.

We would like to emphasize that the connection between the Majorana-like modes here and the symmetry broken Majorana zero modes in topological superconductors has some important consequences. In particular, the Majorana-like modes here will also appear as a zero-bias anomaly in non-superconducting states, similar to Majorana zero modes. In this way, both modes would have similar signatures when probed with scanning tunnel microscopy, appearing as a zero-bias anomaly localized at the edge. These states will however coexist with a gapless background of edge excitations in the bulk. Finally, it is worth mentioning that due to the gapless nature of the bulk excitations, information decoherence in these Majorana-like modes can be different than in conventional Majorana bound states [77–79].

The equivalence between the zero modes of the interacting model and conventional Majorana zero modes can be further emphasized by studying a heterojunction between the interacting model and a topological (trivial) superconductor. The model Hamiltonian of such heterojunction has the following form:

$$\hat{H} = -t \sum_{j=1}^{L-1} \left(\hat{c}_{j+1}^\dagger \hat{c}_j + \hat{c}_j^\dagger \hat{c}_{j+1} \right) -$$
$$V \sum_{j=1}^{L'-1} \left(\hat{c}_{j+1}^\dagger \hat{c}_{j+1} - \frac{1}{2} \right) \left(\hat{c}_j^\dagger \hat{c}_j - \frac{1}{2} \right) +$$
$$\Delta \sum_{j=L'}^{L-1} \left(\hat{c}_{j+1}^\dagger \hat{c}_j^\dagger + \hat{c}_j \hat{c}_{j+1} \right) -$$
$$\mu \sum_{j=1}^{L'} \hat{c}_j^\dagger \hat{c}_j - \mu' \sum_{j=L'+1}^{L} \hat{c}_j^\dagger \hat{c}_j, \quad (8)$$

where Δ and μ' are the order parameter and chemical potential in the topological superconductor, respectively. Here $|\mu'| < 2t$ corresponds to the topological superconductor and $|\mu'| > 2t$ to the trivial one. The local density of states of this system is shown in Figs. 5(c,d). In particular, for an interface between the interacting model and a topological superconductor, no resonance is expected at the junction, as the Majorana zero mode of the topological superconductor and the Majorana-like mode of the interacting model will annihilate each other (Figs. 5(c)).
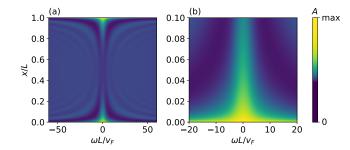
FIG. 6. Local density of states for the continuous wire of interacting fermions normalized on the local density of states of the non-interacting system. (a,b) Color map of $A(x,\omega)$, in the whole chain (a) and close to the edge (b). Here $v_F = g$, the frequency broadening of the local density of states is equal to $\delta = v_F/(2L)$.

In contrast, for the interface between the interacting model and a conventional superconductor, a zero-mode will remain at the interface between the two systems (Figs. 5(d)). Note that the very same phenomenology would be observed if the interacting model is replaced by a symmetry broken topological superconductor.

V. BOSONIZED CONTINUUM LIMIT

In order to show that the peaks exist for an arbitrarily weak attractive interaction we employ bosonization technique for continuous analogue of the model, described by the following Hamiltonian:

$$\hat{H}_c = \int\limits_0^L \left\{ \hat{\psi}^\dagger \left(\frac{\partial_x^2}{2m} - \frac{k_F^2}{2m} \right) \hat{\psi} + \frac{g}{8k_F^2} : [\partial_x \hat{\rho}]^2 : \right\} dx \quad (9)$$

where $\hat{\psi}^\dagger$ and $\hat{\psi}$ are the fermionic creation and annihilation operators, m is the mass of the fermion, k_F is the Fermi momentum, g is the interaction parameter, $\hat{\rho} = \hat{\psi}^\dagger \hat{\psi}$ is the density operator and $: \ldots :$ denotes the normal ordering of the operator. Here we impose zero boundary conditions $\hat{\psi}(0) = \hat{\psi}(L) = 0$. Following Ref. [80] we introduce an auxiliary right moving field $\hat{\psi}_R(x)$ defined on the segment $[-L, L]$:

$$\hat{\psi}(x) = e^{ik_F x} \hat{\psi}_R(x) - e^{-ik_F x} \hat{\psi}_R(-x). \quad (10)$$

Zero boundary conditions for $\hat{\psi}(x)$ are equivalent to periodic ones for $\hat{\psi}_R(x)$ and, hence, the latter field can be straightforwardly bosonized. The Hamiltonian expressed in terms of $\hat{\psi}_R$ has the following form:

$$\hat{H}_c \approx \int\limits_{-L}^L \left[-iv_F \hat{\psi}_R^\dagger \partial_x \hat{\psi}_R - \frac{g}{2} : \hat{\rho}_R(x)\hat{\rho}_R(-x) : \right] dx, \quad (11)$$

where $v_F = k_F/m$, $\hat{\rho}_R = \psi_R^\dagger \psi_R$ and we have replaced the quadratic dispersion by a linear one in the vicinity of the

Fermi surface. The bosonization expression for the field $\hat{\psi}_R(x)$ reads [81]

$$\hat{\psi}_R(x) = \frac{\hat{F}}{\sqrt{2\pi a}} e^{i\pi \hat{N}x/L} e^{i\hat{\phi}(x)}, \quad (12)$$

where $\hat{N}$ is a number operator for extra particles with respect to the Fermi sea state and $\hat{F}$ is the Klein factor $[\hat{N}, \hat{F}] = -\hat{F}$, $\hat{F}^\dagger \hat{F} = \hat{F}\hat{F}^\dagger = 1$. The phase field is given by the following expression:

$$\hat{\phi}(x) = i \sum_{k>0} \sqrt{\frac{\pi}{kL}} \left(e^{-ikx}\hat{b}_k^\dagger - e^{ikx}\hat{b}_k \right) e^{-ka/2}, \quad (13)$$

where $k = \pi j/L$, j is a positive integer, $\hat{b}_k$ and $\hat{b}_k^\dagger$ are the canonical bosonic operators. We also introduce a regularization parameter a and all the expressions are to be understood in the limit $a \to +0$. In terms of the bosonic operators the Hamiltonian is expressed as follows:

$$\hat{H}_c = \sum_{k>0} k \left[v_F \hat{b}_k^\dagger \hat{b}_k - \frac{g}{4\pi} \left(\hat{b}_k \hat{b}_k + \hat{b}_k^\dagger \hat{b}_k^\dagger \right) \right] +$$
$$\frac{\pi}{2L} \left(v_F - \frac{g}{2\pi} \right) \hat{N}^2. \quad (14)$$

This Hamiltonian can be easily diagonalized by the Bogoliubov transform

$$\hat{b}_k = \tilde{b}_k \cosh\varphi + \tilde{b}_k^\dagger \sinh\varphi, \quad \tanh 2\varphi = \frac{g}{2\pi v_F} \quad (15)$$

and reduced to the following form:

$$\hat{H}_c = \sum_{k>0} k \sqrt{v_F^2 - \left(\frac{g}{2\pi}\right)^2} \tilde{b}_k^\dagger \tilde{b}_k + \frac{\pi}{2L} \left(v_F - \frac{g}{2\pi} \right) \hat{N}^2. \quad (16)$$

We note that the Bogoliubov transform can be performed only if $|g| < 2\pi v_F$, otherwise the Hamiltonian (14) is not bounded from below. The case of strong interaction corresponds to the phase separation or charge density wave which cannot be described with the bosonization formalism.

The local density of states of such a wire is given by the following expression:

$$A(x,\omega) = i \int\limits_{-\infty}^\infty \left[G^>(x,x,t) - G^<(x,x,t) \right] e^{i\omega t} dt, \quad (17)$$

where

$$G^>(x,x',t) = -i\langle\hat{\psi}(x,t)\hat{\psi}^\dagger(x',0)\rangle \approx$$
$$G_R^>(x,x',t) + G_R^>(-x,-x',t); \quad (18)$$

$$G_R^>(x,x',t) = -i\langle\hat{\psi}_R(x,t)\hat{\psi}_R^\dagger(x',0)\rangle, \quad (19)$$

and

$$G^<(x,x',t) = i\langle\hat{\psi}^\dagger(x',0)\hat{\psi}(x,t)\rangle \approx$$
$$G_R^<(x,x',t) + G_R^<(-x,-x',t), \quad (20)$$

$$G_R^<(x, x', t) = i\langle \hat{\psi}_R^\dagger(x', 0)\hat{\psi}_R(x, t)\rangle. \qquad (21)$$

Here, in the right hand side of Eqs. (18) and (20) we neglect the terms oscillating as $e^{\pm 2ik_F(x+x')}$. The Green's function of the field $\hat{\psi}_R$ can be evaluated analytically, see Appendix B for details. Figure 6 shows the local density of states of the wire as a function of coordinate and frequency. One can clearly see the peaks at the ends of the wire at zero frequency.

The form (16) of the Hamiltonian allows to evaluate the gap in the local density of states. This gap is equal to $\pi/(2L)[v_F - g/(2\pi)]$ since it is the minimal energy needed to add or remove a single particle to or from the wire without excitation of the bosonic modes. This expression is in the good qualitative agreement with the results shown in the Fig. 3: the peak splitting scales as C/L and the factor C linearly decays with the increase of interaction up to the transition to the phase separation.

VI. SUMMARY

To summarize, we have demonstrated the emergence of zero-bias modes at the edges of a 1D chain of attractively interacting fermions. We have demonstrated that these modes are adiabatically connected to conventional Majorana zero modes of a topological superconductor, yet with the striking difference that they emerge in a situation without gauge symmetry breaking. These many-body zero modes are found to exist at arbitrarily weak attractive interaction and are robust to perturbations which break the integrability of the model, including long-range hopping, interactions, and disorder. In particular, we have demonstrated that these zero-mode resonances can be rationalized both with lattice quantum many-body formalism based on tensor networks, and with a continuum low energy model based on bosonization. Our results put forward a new type of protected zero modes in a purely many-body limit, with no single-particle analog, providing a stepping stone towards the exploration of topological modes in generic quantum disordered many-body systems.

[1] X.-L. Qi and S.-C. Zhang, Topological insulators and superconductors, Rev. Mod. Phys. **83**, 1057 (2011).

[2] M. Sato and Y. Ando, Topological superconductors: a review, Reports on Progress in Physics **80**, 076501 (2017).

[3] S. R. Elliott and M. Franz, Colloquium: Majorana fermions in nuclear, particle, and solid-state physics, Rev. Mod. Phys. **87**, 137 (2015).

[4] D. A. Ivanov, Non-Abelian Statistics of Half-Quantum Vortices in p-Wave Superconductors, Phys. Rev. Lett. **86**, 268 (2001).

[5] A. Y. Kitaev, Fault-tolerant quantum computation by anyons, Annals of Physics **303**, 2 (2003).

[6] C. Nayak, S. H. Simon, A. Stern, M. Freedman, and S. Das Sarma, Non-abelian anyons and topological quantum computation, Rev. Mod. Phys. **80**, 1083 (2008).

[7] M. Sato, Y. Takahashi, and S. Fujimoto, Non-abelian topological order in s-wave superfluids of ultracold fermionic atoms, Phys. Rev. Lett. **103**, 020401 (2009).

[8] J. D. Sau, R. M. Lutchyn, S. Tewari, and S. Das Sarma, Generic new platform for topological quantum computation using semiconductor heterostructures, Phys. Rev. Lett. **104**, 040502 (2010).

[9] J. D. Sau, S. Tewari, R. M. Lutchyn, T. D. Stanescu, and S. Das Sarma, Non-abelian quantum order in spin-orbit-coupled semiconductors: Search for topological majorana particles in solid-state systems, Phys. Rev. B **82**, 214509 (2010).

[10] T. Hyart, B. van Heck, I. C. Fulga, M. Burrello, A. R. Akhmerov, and C. W. J. Beenakker, Flux-controlled quantum computation with Majorana fermions, Phys. Rev. B **88**, 035121 (2013).

[11] T. Karzig, C. Knapp, R. M. Lutchyn, P. Bonderson, M. B. Hastings, C. Nayak, J. Alicea, K. Flensberg, S. Plugge, Y. Oreg, C. M. Marcus, and M. H. Freedman, Scalable designs for quasiparticle-poisoning-protected topological quantum computation with Majorana zero modes, Phys. Rev. B **95**, 235305 (2017).

[12] R. M. Lutchyn, E. P. A. M. Bakkers, L. P. Kouwenhoven, P. Krogstrup, C. M. Marcus, and Y. Oreg, Majorana zero modes in superconductor-semiconductor heterostructures, Nature Reviews Materials **3**, 52 (2018).

[13] C. W. J. Beenakker, Search for non-Abelian Majorana braiding statistics in superconductors, SciPost Phys. Lect. Notes , 15 (2020).

[14] R. M. Lutchyn, J. D. Sau, and S. Das Sarma, Majorana fermions and a topological phase transition in semiconductor-superconductor heterostructures, Phys. Rev. Lett. **105**, 077001 (2010).

[15] Y. Oreg, G. Refael, and F. von Oppen, Helical Liquids and Majorana Bound States in Quantum Wires, Phys. Rev. Lett. **105**, 177002 (2010).

[16] T. D. Stanescu, R. M. Lutchyn, and S. Das Sarma, Majorana fermions in semiconductor nanowires, Phys. Rev. B **84**, 144522 (2011).

[17] V. Mourik, K. Zuo, S. M. Frolov, S. R. Plissard, E. P. A. M. Bakkers, and L. P. Kouwenhoven, Signatures of Majorana fermions in hybrid superconductor-semiconductor nanowire devices, Science **336**, 1003 (2012).

[18] A. D. K. Finck, D. J. Van Harlingen, P. K. Mohseni, K. Jung, and X. Li, Anomalous modulation of a zero-bias peak in a hybrid nanowire-superconductor device, Phys. Rev. Lett. **110**, 126406 (2013).

[19] H. O. H. Churchill, V. Fatemi, K. Grove-Rasmussen, M. T. Deng, P. Caroff, H. Q. Xu, and C. M. Marcus, Superconductor-nanowire devices from tunneling to the multichannel regime: Zero-bias oscillations and magnetoconductance crossover, Phys. Rev. B **87**, 241401 (2013).

[20] D. Rainis, L. Trifunovic, J. Klinovaja, and D. Loss, Towards a realistic transport modeling in a superconducting nanowire with Majorana fermions, Phys. Rev. B **87**, 024515 (2013).

[21] A. E. Antipov, A. Bargerbos, G. W. Winkler, B. Bauer, E. Rossi, and R. M. Lutchyn, Effects of Gate-Induced Electric Fields on Semiconductor Majorana Nanowires, Phys. Rev. X **8**, 031041 (2018).

[22] T. Karzig, G. Refael, and F. von Oppen, Boosting majorana zero modes, Phys. Rev. X **3**, 041017 (2013).

[23] T.-P. Choy, J. M. Edge, A. R. Akhmerov, and C. W. J. Beenakker, Majorana fermions emerging from magnetic nanoparticles on a superconductor without spin-orbit coupling, Phys. Rev. B **84**, 195442 (2011).

[24] S. Nadj-Perge, I. K. Drozdov, B. A. Bernevig, and A. Yazdani, Proposal for realizing Majorana fermions in chains of magnetic atoms on a superconductor, Phys. Rev. B **88**, 020407 (2013).

[25] S. Nadj-Perge, I. K. Drozdov, J. Li, H. Chen, S. Jeon, J. Seo, A. H. MacDonald, B. A. Bernevig, and A. Yazdani, Observation of Majorana fermions in ferromagnetic atomic chains on a superconductor, Science **346**, 602 (2014).

[26] A. Heimes, P. Kotetes, and G. Schön, Majorana fermions from Shiba states in an antiferromagnetic chain on top of a superconductor, Phys. Rev. B **90**, 060507 (2014).

[27] L. Fu and C. L. Kane, Superconducting Proximity Effect and Majorana Fermions at the Surface of a Topological Insulator, Phys. Rev. Lett. **100**, 096407 (2008).

[28] L. Fu and C. L. Kane, Josephson current and noise at a superconductor/quantum-spin-Hall-insulator/superconductor junction, Phys. Rev. B **79**, 161408 (2009).

[29] J. R. Williams, A. J. Bestwick, P. Gallagher, S. S. Hong, Y. Cui, A. S. Bleich, J. G. Analytis, I. R. Fisher, and D. Goldhaber-Gordon, Unconventional Josephson Effect in Hybrid Superconductor-Topological Insulator Devices, Phys. Rev. Lett. **109**, 056803 (2012).

[30] S. Hart, H. Ren, T. Wagner, P. Leubner, M. Mühlbauer, C. Brüne, H. Buhmann, L. W. Molenkamp, and A. Yacoby, Induced superconductivity in the quantum spin Hall edge, Nature Physics **10**, 638 (2014).

[31] V. S. Pribiag, A. J. A. Beukman, F. Qu, M. C. Cassidy, C. Charpentier, W. Wegscheider, and L. P. Kouwenhoven, Edge-mode superconductivity in a two-dimensional topological insulator, Nature Nanotechnology **10**, 593 (2015).

[32] H. Ren, F. Pientka, S. Hart, A. T. Pierce, M. Kosowsky, L. Lunczer, R. Schlereth, B. Scharf, E. M. Hankiewicz, L. W. Molenkamp, B. I. Halperin, and A. Yacoby, Topo-logical superconductivity in a phase-controlled Josephson junction, Nature **569**, 93 (2019).

[33] A. Fornieri, A. M. Whiticar, F. Setiawan, E. Portolés, A. C. C. Drachmann, A. Keselman, S. Gronin, C. Thomas, T. Wang, R. Kallaher, G. C. Gardner, E. Berg, M. J. Manfra, A. Stern, C. M. Marcus, and F. Nichele, Evidence of topological superconductivity in planar Josephson junctions, Nature **569**, 89 (2019).

[34] P. San-Jose, J. L. Lado, R. Aguado, F. Guinea, and J. Fernández-Rossier, Majorana zero modes in graphene, Phys. Rev. X **5**, 041042 (2015).

[35] Y. Li, M. Amado, T. Hyart, G. P. Mazur, V. Risinggård, T. Wagner, L. McKenzie-Sell, G. Kimbell, J. Wunderlich, J. Linder, and J. W. A. Robinson, Transition between canted antiferromagnetic and spin-polarized ferromagnetic quantum hall states in graphene on a ferrimagnetic insulator, Phys. Rev. B **101**, 241405 (2020).

[36] L. Veyrat, C. Déprez, A. Coissard, X. Li, F. Gay, K. Watanabe, T. Taniguchi, Z. Han, B. A. Piot, H. Sellier, and B. Sacépé, helical quantum hall phase in graphene on srtio3, .

[37] M. Ezawa, Antiferromagnetic Topological Superconductor and Electrically Controllable Majorana Fermions, Phys. Rev. Lett. **114**, 056403 (2015).

[38] J. L. Lado and M. Sigrist, Two-dimensional topological superconductivity with antiferromagnetic insulators, Phys. Rev. Lett. **121**, 037002 (2018).

[39] S. Kezilebieke, M. Nurul Huda, V. Vaňo, M. Aapro, S. C. Ganguli, O. J. Silveira, S. Głodzik, A. S. Foster, T. Ojanen, and P. Liljeroth, Topological superconductivity in a designer ferromagnet-superconductor van der Waals heterostructure, arXiv e-prints , arXiv:2002.02141 (2020), arXiv:2002.02141 [cond-mat.mes-hall].

[40] A. Y. Kitaev, Unpaired majorana fermions in quantum wires, Physics-Uspekhi **44**, 131–136 (2001).

[41] E. M. Stoudenmire, J. Alicea, O. A. Starykh, and M. P. Fisher, Interaction effects in topological superconducting wires supporting Majorana fermions, Phys. Rev. B **84**, 014503 (2011).

[42] M. Tezuka and N. Kawakami, Reentrant topological transitions in a quantum wire/superconductor system with quasiperiodic lattice modulation, Phys. Rev. B **85**, 140508 (2012).

[43] R. Thomale, S. Rachel, and P. Schmitteckert, Tunneling spectra simulation of interacting majorana wires, Phys. Rev. B **88**, 161103 (2013).

[44] S. Gangadharaiah, B. Braunecker, P. Simon, and D. Loss, Majorana edge states in interacting one-dimensional systems, Phys. Rev. Lett. **107**, 036801 (2011).

[45] A. Haim, A. Keselman, E. Berg, and Y. Oreg, Time-reversal-invariant topological superconductivity induced by repulsive interactions in quantum wires, Phys. Rev. B **89**, 220504 (2014).

[46] M. Cheng, M. Becker, B. Bauer, and R. M. Lutchyn, Interplay between kondo and majorana interactions in quantum dots, Phys. Rev. X **4**, 031051 (2014).

[47] A. M. Lobos, R. M. Lutchyn, and S. Das Sarma, Interplay of disorder and interaction in majorana quantum wires, Phys. Rev. Lett. **109**, 146403 (2012).

[48] E. M. Stoudenmire, J. Alicea, O. A. Starykh, and M. P. Fisher, Interaction effects in topological superconducting wires supporting majorana fermions, Phys. Rev. B **84**, 014503 (2011).

[49] S. V. Aksenov, A. O. Zlotnikov, and M. S. Shustin, Strong coulomb interactions in the problem of majorana modes in a wire of the nontrivial topological class bdi, Phys. Rev. B **101**, 125431 (2020).

[50] A. Keselman and E. Berg, Gapless symmetry-protected topological phase of fermions in one dimension, Phys. Rev. B **91**, 235309 (2015).

[51] L. Fidkowski, R. M. Lutchyn, C. Nayak, and M. P. A. Fisher, Majorana zero modes in one-dimensional quantum wires without long-ranged superconducting order, Phys. Rev. B **84**, 195436 (2011).

[52] J. D. Sau, B. I. Halperin, K. Flensberg, and S. Das Sarma, Number conserving theory for topologically protected degeneracy in one-dimensional fermions, Phys. Rev. B **84**, 144509 (2011).

[53] D. E. Parker, T. Scaffidi, and R. Vasseur, Topological luttinger liquids from decorated domain walls, Phys. Rev. B **97**, 165114 (2018).

[54] N. Lang and H. P. Büchler, Topological states in a microscopic model of interacting fermions, Phys. Rev. B **92**, 041118 (2015).

[55] T. Scaffidi, D. E. Parker, and R. Vasseur, Gapless symmetry-protected topological order, Phys. Rev. X **7**, 041048 (2017).

[56] R. Verresen, N. G. Jones, and F. Pollmann, Topology and edge modes in quantum critical chains, Phys. Rev. Lett. **120**, 057001 (2018).

[57] A. Keselman, E. Berg, and P. Azaria, From one-dimensional charge conserving superconductors to the gapless haldane phase, Phys. Rev. B **98**, 214501 (2018).

[58] J. Ruhman, E. Berg, and E. Altman, Topological states in a one-dimensional fermi gas with attractive interaction, Phys. Rev. Lett. **114**, 100401 (2015).

[59] G. Ortiz, J. Dukelsky, E. Cobanera, C. Esebbag, and C. Beenakker, Many-body characterization of particle-conserving topological superfluids, Phys. Rev. Lett. **113**, 267002 (2014).

[60] J. Alicea, New directions in the pursuit of majorana fermions in solid state systems, Reports on Progress in Physics **75**, 076501 (2012).

[61] P. C. Hohenberg, Existence of long-range order in one and two dimensions, Phys. Rev. **158**, 383 (1967).

[62] N. D. Mermin and H. Wagner, Absence of ferromagnetism or antiferromagnetism in one- or two-dimensional isotropic heisenberg models, Phys. Rev. Lett. **17**, 1133 (1966).

[63] F. C. Alcaraz, M. N. Barber, M. T. Batchelor, R. J. Baxter, and G. R. W. Quispel, Surface exponents of the quantum XXZ, Ashkin-Teller and Potts models, Journal of Physics A: Mathematical and General **20**, 6397–6409 (1987).

[64] E. K. Sklyanin, Boundary conditions for integrable quantum systems, Journal of Physics A: Mathematical and General **21**, 2375–2389 (1988).

[65] H. Mikeska and A. Kolezhuk, One-dimensional magnetism, Lect. Notes. Phys. **645** (2004).

[66] P. Fendley, Strong zero modes and eigenstate phase transitions in the xyz/interacting majorana chain, Journal of Physics A: Mathematical and Theoretical **49**, 30LT01 (2016).

[67] S.-i. Tomonaga, Remarks on Bloch's Method of Sound Waves applied to Many-Fermion Problems, Progress of Theoretical Physics **5**, 544 (1950), https://academic.oup.com/ptp/article-pdf/5/4/544/5430161/5-4-544.pdf.

[68] J. Luttinger, An exactly soluble model of a many-fermion system, Journal of mathematical physics **4**, 1154 (1963).

[69] F. D. M. Haldane, 'luttinger liquid theory' of one-dimensional quantum fluids. i. properties of the luttinger model and their extension to the general 1d interacting spinless fermi gas, Journal of Physics C: Solid State Physics **14**, 2585–2609 (1981).

[70] A. Weiße, G. Wellein, A. Alvermann, and H. Fehske, The kernel polynomial method, Rev. Mod. Phys. **78**, 275 (2006).

[71] F. A. Wolf, J. A. Justiniano, I. P. McCulloch, and U. Schollwöck, Spectral functions and time evolution from the chebyshev recursion, Phys. Rev. B **91**, 115144 (2015).

[72] J. L. Lado and O. Zilberberg, Topological spin excitations in harper-heisenberg spin chains, Phys. Rev. Research **1**, 033009 (2019).

[73] J. L. Lado and M. Sigrist, Solitonic in-gap modes in a superconductor-quantum antiferromagnet interface, Phys. Rev. Research **2**, 023347 (2020).

[74] M. Fishman, S. R. White, and E. M. Stoudenmire, The ITensor Software Library for Tensor Network Calculations, arXiv:2007.14822.

[75] ITensor Library http://itensor.org.

[76] DMRGpy Library https://github.com/joselado/dmrgpy.

[77] D. Rainis and D. Loss, Majorana qubit decoherence by quasiparticle poisoning, Phys. Rev. B **85**, 174533 (2012).

[78] M. J. Schmidt, D. Rainis, and D. Loss, Decoherence of majorana qubits by noisy gates, Phys. Rev. B **86**, 085414 (2012).

[79] J. C. Budich, S. Walter, and B. Trauzettel, Failure of protection of majorana based qubits against decoherence, Phys. Rev. B **85**, 121405 (2012).

[80] M. Fabrizio and A. O. Gogolin, Interacting one-dimensional electron gas with open boundaries, Phys. Rev. B **51**, 17827 (1995).

[81] J. Von Delft and H. Schoeller, Bosonization for beginners—refermionization for experts, Annalen der Physik **7**, 225 (1998).

[82] E. Casiano-Diaz, Quantum entanglement of one-dimensional spinless fermions, (2019).

[83] M. Greiter, V. Schnells, and R. Thomale, The 1D Ising model and the topological phase of the Kitaev chain, Annals of Physics **351**, 1026 (2014), arXiv:1402.5262.

Appendix A: Critical point

In the general interacting case the Bethe ansatz expression for the ground state of the system is complicated except for the critical point $\mu = 0$, $V = 2t$. In this case the ground state has the form [82]

$$|\Psi_0\rangle = \frac{1}{2^{L/2}} \prod_{j=1}^{L} \left(1 + \hat{c}_j^\dagger \right) |0\rangle \tag{A1}$$

corresponding to energy $E_0 = t(1 - L)/2$. Interestingly, this is actually same ground state as in Kitaev model, and thus it would be possible to construct Majorana operators describing localized zero-energy excitations [83]. It must be noted that in the present model there will

be also additional low-energy excitations as we are considering a truly interacting model instead of mean-field Hamiltonian.

In order to prove this result we define $|\Psi_{j-1}\rangle$ be defined as

$$|\Psi_{j-1}\rangle = \frac{1}{2^{L/2}} \prod_{k=j}^{L} \left(1 + \hat{c}_k^\dagger\right) |0\rangle. \tag{A2}$$

At the same time we define $\hat{H}_{j-1}$ as:

$$\hat{H}_{j-1} = -t \sum_{k=j}^{L-1} \left(\hat{c}_{k+1}^\dagger \hat{c}_k + \hat{c}_k^\dagger \hat{c}_{k+1}\right) - $$
$$2t \sum_{k=j}^{L-1} \left(\hat{c}_{k+1}^\dagger \hat{c}_{k+1} - \frac{1}{2}\right) \left(\hat{c}_k^\dagger \hat{c}_k - \frac{1}{2}\right). \tag{A3}$$

It's obvious that $\hat{H}_0 = \hat{H}_I$ at $V = 2t$ and $\mu = 0$. We are going to prove that $|\Psi_{j-1}\rangle$ is the eigenstate of the Hamiltonian $\hat{H}_{j-1}$ with the energy $t(j-L)/2$. For $j = L$ this fact is obvious because $\hat{H}_{L-1} = 0$. Assume that for some $j-1$ this statement is true. Then let us prove it for $j-2$:

$$\hat{H}_{j-2}|\Psi_{j-2}\rangle = \left[-t\left(\hat{c}_j^\dagger \hat{c}_{j-1} + \hat{c}_{j-1}^\dagger \hat{c}_j\right) - 2t\left(\hat{c}_j^\dagger \hat{c}_j - \frac{1}{2}\right)\left(\hat{c}_{j-1}^\dagger \hat{c}_{j-1} - \frac{1}{2}\right) + \hat{H}_j\right]\left(1 + \hat{c}_{j-1}^\dagger\right)|\Psi_{j-1}\rangle =$$
$$\frac{t(j-L)}{2}|\Psi_{j-2}\rangle - t\left[\hat{c}_{j-1}^\dagger|\Psi_j\rangle - \left(\hat{c}_j^\dagger \hat{c}_j - \frac{1}{2}\right)|\Psi_{j-1}\rangle + \hat{c}_j^\dagger \hat{c}_{j-1} \hat{c}_{j-1}^\dagger |\Psi_{j-1}\rangle + $$
$$2\left(\hat{c}_j^\dagger \hat{c}_j - \frac{1}{2}\right)\left(\hat{c}_{j-1}^\dagger \hat{c}_{j-1} - \frac{1}{2}\right)\hat{c}_{j-1}^\dagger |\Psi_{j-1}\rangle\right] =$$
$$\frac{t(j-L)}{2}|\Psi_{j-2}\rangle - t\left[\hat{c}_{j-1}^\dagger|\Psi_j\rangle - \hat{c}_j^\dagger|\Psi_j\rangle + \frac{1}{2}|\Psi_{j-1}\rangle + \hat{c}_j^\dagger|\Psi_j\rangle + \left(\hat{c}_j^\dagger \hat{c}_j - \frac{1}{2}\right)\hat{c}_{j-1}^\dagger|\Psi_{j-1}\rangle\right] =$$
$$\frac{t(j-L)}{2}|\Psi_{j-2}\rangle - t\left[\hat{c}_{j-1}^\dagger|\Psi_j\rangle + \frac{1}{2}|\Psi_{j-1}\rangle + \hat{c}_{j-1}^\dagger \hat{c}_j^\dagger|\Psi_j\rangle - \frac{1}{2}\hat{c}_{j-1}^\dagger|\Psi_{j-1}\rangle\right] =$$
$$\frac{t(j-L)}{2}|\Psi_{j-2}\rangle - t\left[\frac{1}{2}|\Psi_{j-1}\rangle + \frac{1}{2}\hat{c}_{j-1}^\dagger|\Psi_{j-1}\rangle\right] = \frac{t(j-1-L)}{2}|\Psi_{j-2}\rangle. \tag{A4}$$

In order to prove that the found eigenstate is the ground state, i.e. has the minimal possible energy, we notice that the Hamiltonian can be written as:

$$\hat{H}_I = -t \sum_{j=1}^{L-1} \left[\hat{c}_{j+1}^\dagger \hat{c}_j + \hat{c}_j^\dagger \hat{c}_{j+1} + \right.$$
$$\left. 2\left(\hat{c}_{j+1}^\dagger \hat{c}_{j+1} - \frac{1}{2}\right)\left(\hat{c}_j^\dagger \hat{c}_j - \frac{1}{2}\right)\right] \tag{A5}$$

Each term of the sum has the lowest eigenvalue equal to $-t/2$ and there are $L-1$ terms total, then the energy of the ground state cannot be lower than $t(1-L)/2$.

Since the state $|\Psi_0\rangle$ is not an eigenstate of the number of particles operator, one can project it onto the subspaces with the fixed number of particles yielding $L+1$-times degenerate ground states corresponding to the different number of particles N from 0 to L:

$$|\Psi_{0N}\rangle = \frac{2^{L/2}}{\sqrt{\binom{L}{N}}} \hat{P}_N|\Psi_0\rangle, \tag{A6}$$

where $\hat{P}_N$ is an orthogonal projector onto the subspace with N particles.

Appendix B: Green's functions of the continuous wire

The greater and lesser Green's functions of the field $\hat{\psi}_R$ are equal to

$$G_R^>(x, x', t) = $$
$$-\frac{i}{2\pi a}\left\langle \hat{F}(t) e^{i\pi \hat{N}(x-x')/L} \hat{F}^\dagger e^{i\hat{\phi}(x,t)} e^{-i\hat{\phi}(x')}\right\rangle; \tag{B1}$$

$$G_R^<(x, x', t) =$$
$$\frac{i}{2\pi a} \left\langle e^{-i\pi \hat{N}x'/L} \hat{F}^\dagger \hat{F}(t) e^{i\pi \hat{N}x/L} e^{-i\hat{\phi}(x')} e^{i\hat{\phi}(x,t)} \right\rangle, \quad \text{(B2)}$$

where $\hat{F}(t) = e^{i\hat{H}_c t}\hat{F}e^{-i\hat{H}_c t}$ and $\hat{\phi}(x,t) = e^{i\hat{H}_c t}\hat{\phi}(x)e^{-i\hat{H}_c t}$. After a long but straightforward calculations one obtains:

$$G_R^>(x, x', t) = -\frac{ic}{2L} \exp\left[-\frac{i\pi t}{2L}\left(v_F - \frac{g}{2\pi}\right) + \frac{i\pi(x-x')}{L} \right] \times$$

$$\frac{\left[1 - e^{-\frac{\pi}{L}(a+i\tilde{v}_F t + ix + ix')}\right]^{\frac{s}{2}} \left[1 - e^{-\frac{\pi}{L}(a+i\tilde{v}_F t - ix - ix')}\right]^{\frac{s}{2}} \left[1 - e^{-\frac{\pi}{L}(a+i\tilde{v}_F t + ix - ix')}\right]^{\frac{1-c}{2}}}{\left|1 - e^{-\frac{\pi}{L}(a-2ix)}\right|^{\frac{s}{2}} \left|1 - e^{-\frac{\pi}{L}(a-2ix')}\right|^{\frac{s}{2}} \left[1 - e^{-\frac{\pi}{L}(a+i\tilde{v}_F t - ix + ix')}\right]^{\frac{1+c}{2}}}; \quad \text{(B3)}$$

$$G_R^<(x, x', t) = \frac{ic}{2L} \exp\left[\frac{i\pi t}{2L}\left(v_F - \frac{g}{2\pi}\right) \right] \times$$

$$\frac{\left[1 - e^{-\frac{\pi}{L}(a-i\tilde{v}_F t - ix - ix')}\right]^{\frac{s}{2}} \left[1 - e^{-\frac{\pi}{L}(a-i\tilde{v}_F t + ix + ix')}\right]^{\frac{s}{2}} \left[1 - e^{-\frac{\pi}{L}(a-i\tilde{v}_F t - ix + ix')}\right]^{\frac{1-c}{2}}}{\left|1 - e^{-\frac{\pi}{L}(a+2ix)}\right|^{\frac{s}{2}} \left|1 - e^{-\frac{\pi}{L}(a+2ix')}\right|^{\frac{s}{2}} \left[1 - e^{-\frac{\pi}{L}(a-i\tilde{v}_F t + ix - ix')}\right]^{\frac{1+c}{2}}}, \quad \text{(B4)}$$

where $c = \cosh 2\varphi$, $s = \sinh 2\varphi$ and $\tilde{v}_F = \sqrt{v_F^2 - g^2/(2\pi)^2}$. Finally, the expression for the local density of states reads as:

$$A(x, \omega) = 2 \int_{-\infty}^{+\infty} e^{i\omega t} \, \text{Re}\left\{ e^{-\frac{i\pi t}{2L}\left(v_F - \frac{g}{2\pi}\right)} \frac{\left(1 - e^{-\frac{\pi a}{L}}\right)^c \left[1 - e^{-\frac{\pi}{L}(a-i\tilde{v}_F t - 2ix)}\right]^{\frac{s}{2}} \left[1 - e^{-\frac{\pi}{L}(a-i\tilde{v}_F t + 2ix)}\right]^{\frac{s}{2}}}{\pi a \left|1 - e^{-\frac{\pi}{L}(a+2ix)}\right|^s \left[1 - e^{-\frac{\pi}{L}(a-iv_F t)}\right]^c} \right\} dt. \quad \text{(B5)}$$

Appendix C: Persistent current in a ring

We close up the chain into a ring with a weak link and pierce it with a magnetic flux. The Hamiltonian of such a system reads as:

$$\hat{H}_I' = \hat{H}_I - t_w \left(\hat{c}_L^\dagger \hat{c}_1 e^{i\Phi} + \hat{c}_1^\dagger \hat{c}_L e^{-i\Phi} \right), \quad \text{(C1)}$$

where t_w is hopping parameter through the weak link between the first and the last sites of the chain, and Φ determines the flux in the units of $\Phi_0/(2\pi)$, where Φ_0 is the normal (not superconducting) flux quantum. The current operator is defined as

$$\hat{J} = \frac{\partial \hat{H}_I'}{\partial \Phi} = -it_w \left(\hat{c}_L^\dagger \hat{c}_1 e^{i\Phi} - \hat{c}_1^\dagger \hat{c}_L e^{-i\Phi} \right). \quad \text{(C2)}$$

The current dependence on the flux is shown in Fig. 7(a), (b) for different values of interaction strength. The dis-continuities in the current-flux relation correspond to the number of particles switches in the ring. Figures 7(c) and (d) show the local density of states at the site adjacent to the weak link as a function of flux and frequency. The peak splitting oscillates as a function of flux, the number of particles switches take place exactly at the peak's intersections. The behavior of the current and spectral function at the critical point $V = 2t$ mostly resembles the behavior of the mean field Kitaev model where these quantities are π-periodic with the flux if one allows parity switches, and 2π periodic if the parity is kept fixed. Away from the critical point we do not observe exact π-periodicity of the current in the presence of parity switches which may be a consequence of a finite overlap of the peaks through the bulk of the chain.
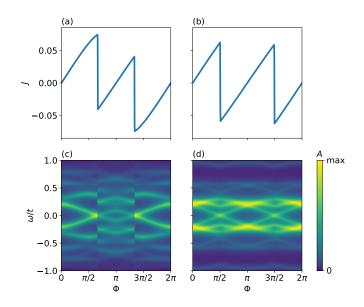
FIG. 7. (a), (b) The persistent current in the ring as a function of flux. (c), (d) The spectral function at the site adjacent to the weak link as a function of frequency and flux. The parameters are $t_w = 0.2t$, $L = 10$, $\mu = 0$, (a), (c) $V = 1.5t$, (b), (d) $V = 2t$. The data is obtained using exact diagonalization of the Hamiltonian (C1). The frequency broadening of the local density of states is equal to $\delta = 0.05t$.